Robust Control with Dynamic Compensation for Human-Wheelchair System

Víctor H. Andaluz[1], Paúl Canseco[1], José Varela[1], Jessica S. Ortiz[1], María G. Pérez[1], Flavio Roberti[2], and Ricardo Carelli[2]

[1] FISEI, Universidad Técnica de Ambato, Ambato-Ecuador
victorhandaluz@uta.edu.ec
[2] Instituto de Automática, Universidad Nacional de San Juan, San Juan-Argentina
vandaluz@inaut.unsj.edu.ar

Abstract. This work presents the kinematic and dynamic modeling of a human-wheelchair system, and dynamic control to solve the path following problem. First it is proposed a dynamic modeling of the human-wheelchair system where it is considered that its mass center is not located at the center the wheels' axle of the wheelchair. Then, the design of the control algorithm is presented. This controller design is based on two cascaded subsystems: a kinematic controller with command saturation, and a dynamic controller that compensates the dynamics of the robot. Stability and robustness are proved by using Lyapunov's method. Experimental results show a good performance of the proposed controller as proved by the theoretical design.

Keywords: Human-wheelchair system, dynamic control and dynamic modeling.

1 Introduction

In recent years, robotics research has experienced a significant change. The research interests are moving from the development of robots for structured industrial environments to the development of autonomous mobile robots operating in unstructured and natural environments. These autonomous robots are applicable in a number of challenging tasks such as cleaning of hazardous material, surveillance, rescue and reconnaissance in unstructured environments which humans are kept away from. Since it is foreseen that this new class of mobile robots will have extensive applications in activities where human capabilities are needed, they have attracted the attention of robotics researchers [1-3].

Therefore, the necessity of technological development in the field of medical and welfare equipment is cried out. By responding to this issue, different types of technologies have been developing by Engineering for the assistance of human [4-7]. Electrical wheelchair is an important means of transport for handicapped and aged people, who do not have the capability of walking, normally can move around using a commercially available wheelchair. However there are many people suffering from

X. Zhang et al. (Eds.): ICIRA 2014, Part I, LNAI 8917, pp. 376–389, 2014.

severe loss of motor function due to variety of accidents or diseases such as a Spinal Cord Injury (SCI) or Amyotrophic Lateral Sclerosis (ALS), in this cases is necessary to provide a new way to command such an electrical vehicle.

Human Machine Interface (HMI) based on electro-biological signal are present in [1,4,8,9]. Such interfaces allow commanding wheelchair robot governed by a computer. The literature shows that an autonomous wheelchair can be successfully driven by persons using only electrical signals generated by eye-blinks, voice, and others [1,2,10,11]. Then, a trajectory will be automatically generated and a trajectory tracking control will guide the wheelchair to the desired target. As indicated, the fundamental problems of motion control of wheelchair robots can be roughly classified in three groups [12]: 1) *point stabilization*: the goal is to stabilize the wheelchair at a given target point, with a desired orientation; 2) *trajectory tracking*: the wheelchair is required to track a time parameterized reference; and 3) *path following*: the wheelchair is required to converge to a path and follow it, without any time specifications; this work is focused to resolve the path following problem.

The path following problem has been well studied and many solutions have been proposed and applied in a wide range of applications. Let $\mathcal{P}_d(s) \in \Re^2$ be a desired geometric path parameterized by the curvilinear abscissa $s \in \Re$. In the literature is common to find different control algorithms for path following where is conseder $s(t)$ as an additional control input. In [13-16], the rate of progression ($\dot{s}$) of a virtual vehicle has been controlled explicitly. Another method for path following of wheelchair robot is the image-based control. The main objective of this method is to detect and follow the desired path through vision sensors [3]. Furthermore, it is important to consider the wheelchair's dynamics in addition to its kinematics because wheelchairs carry relatively heavy loads. As an example, the trajectory tracking task can be severely affected by the change imposed to the wheelchair dynamics when it is carrying a person, as shown in [17]. Hence, some path following control architectures already proposed in the literature have considered the dynamics of the wheelchair robots [11,19].

In such context, this work proposes a new method to solve the path following problem for a wheelchair robot to assist persons with severe motor diseases. Additionally, it is proposed a dynamic modeling of the human-wheelchair system which, which has reference velocities as input signals to the wheelchair, as it is common in commercial robots, and it also has adequate structure for control law designing [11]. The proposed control scheme is divided into two subsystems, each one being a controller itself: 1) the firts on is a kinematic controller with saturation of velocity commands, which is based on the wheelchair robot's kinematic. The path following problem is addressed in this subsystem. It is worth noting that the proposed controller does not consider $s(t)$ as an additional control input as it is frequent in literature; and 2) an dynamic compensation controller that considered the human-wheelchair system dynamic model, which are directly related to physical parameters of the system. In addition, both stability and robustness properties to parametric uncertainties in the dynamic model are proven through Lyapunov's method. To validate the proposed control algorithm, experimental results are included and discussed.

The paper is organized as follows: Section 2 shown the complete dynamic modeling of the human-wheelchair system, while Section 3 describes the path

following's formulation problem and it also presents the controllers design. Furthermore, the analysis of the system's stability is developed. Next, experimental results are presented and discussed in Section 4, and finally the conclusions are given in Section 5.

2 Human-Wheelchair System Modeling

The wheelchair robot used in this work presents similar characteristics to that of a unicycle-like mobile robot, because it has two driven wheels which are controlled independently by two D.C. motors and four caster wheel to maintain balance. The unicycle-type mobile robots have a caster wheel to maintain stability, but in this work the wheelchair has four caster wheels around the central axis conferring greater stability to the human-wheelchair system. The dynamic modeling of the human-wheelchair system is developed in this section, considering a horizontal work plane where the wheelchair moves. The wheelchair type unicycle-like mobile robot presents the advantages of high mobility, high traction with pneumatic tires, and a simple wheel configuration.

2.1 Kinematic Model

It is assumed that the mobile platform moves on a planar horizontal surface. Let $R(X, Y, Z)$ be any fixed frame with Z vertical, as the Fig.1 shows.

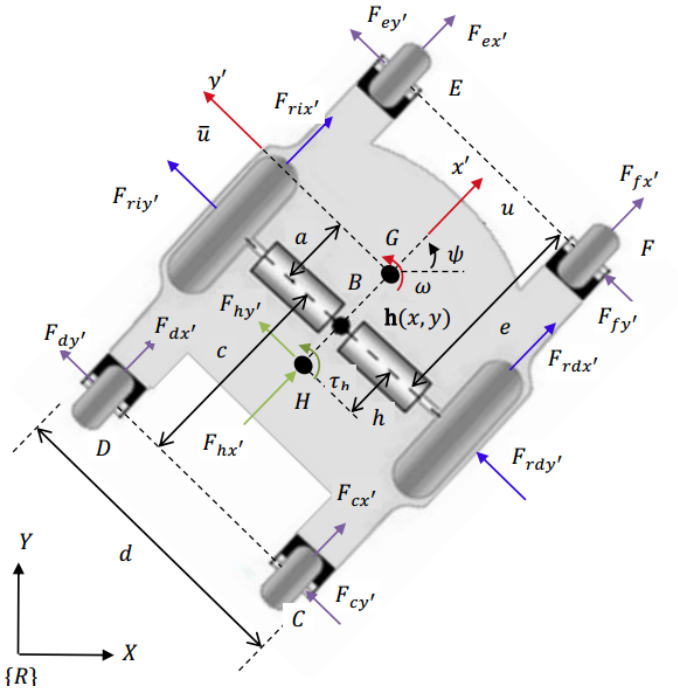

Fig. 1. Schematic of the wheelchair

This work is based on Unicycle-like wheelchair. A unicycle wheelchair is a driving robot that can rotate freely around its axis. The term unicycle is often used in robotics to mean a generalized cart or car moving in a two-dimensional world; these are also often called unicycle-like or unicycle-type vehicles. On the other hand, the non-holonomic velocity constraint of the wheelchair determines that it can only move perpendicular to the wheels axis,

$$\dot{x}sen(\psi) - \dot{y}\cos(\psi) + a\dot{\psi} = 0 \tag{1}$$

Therefore, the configuration instantaneous kinematic model of the holonomic mobile platform is defined as,

$$\begin{cases} \dot{x} = ucos\psi - a\omega sen\psi \\ \dot{y} = usen\psi + a\omega cos\psi \\ \dot{\psi} = \omega \end{cases} \tag{2}$$

Equation (2) can be written in compact form as

$$\dot{\mathbf{h}} = \mathbf{J}(\psi)\mathbf{v} \tag{3}$$

$$\dot{\psi} = \omega$$

where $\dot{\mathbf{h}} = [\dot{x} \quad \dot{y}]^T \in \mathcal{R}^2$ represents the vector of axis velocity; $\mathbf{J}(\psi) \in \mathcal{R}^{2x2}$ is a singular matrix; and the control (*of manoeuvrability*) of the wheelchair is defined $\mathbf{v} = [u \quad \omega]^T \in \mathcal{R}^2$ in which u and ω which represent the linear and angular velocities of the wheelchair, respectively.

2.2 Dynamic Model

Fig.1 illustrates the wheelchair considering in this work; the position of the human-wheelchair system, is given by point G, representing the center of mass; $\mathbf{h} = [x \quad y]^T$ represents the point that is required to track a path in $\mathcal{R}$; ψ is the orientation of the wheelchair. On the other hand, u' and $\bar{u}$ are the longitudinal and lateral velocities of the center of mass; ω is the angular velocity; *a, c, e, d,* and *h* are distances; $F_{rdx'}$ and $F_{rdy'}$ are the longitudinal and lateral tire forces of the right wheel; $F_{rix'}$ and $F_{riy'}$ are the longitudinal and lateral tire forces of the left wheel; $F_{cx'}$ $F_{cy'}$ $F_{dx'}$, $F_{dy'}$ $F_{ex'}$, $F_{ey'}$, $F_{fx'}$ and $F_{fy'}$ are the longitudinal and lateral tire forces exerted on *C, D, E* and *F* by the castor wheels; $F_{hx'}$ and $F_{hy'}$ are the longitudinal and lateral force exerted on E by the human; and τ_h τ_e is the moment exerted by the human.

The force and moment equations for the mobile robot are:

$$\sum F_{x'} = m(\dot{u} - \bar{u}\omega) = F_{rdx'} + F_{rix'} + F_{hx'} + F_{cx'} + F_{dx'} + F_{ex'} + F_{fx'} \tag{4}$$

$$\sum F_{y'} = m\left(\dot{\bar{u}} - u\omega\right) = F_{rdy'} + F_{riy'} + F_{hy'} + F_{cy'} + F_{dy'} + F_{ey'} + F_{fy'} \tag{5}$$

$$\sum M_z = I_z\dot{\omega} = \frac{d}{2}(F_{rdx'} - F_{rix'}) - a\left(F_{rdy'} + F_{riy'}\right) - (h+a)F_{hx'} - (c + a)\left(F_{dy'} + F_{cy'}\right) + (e-a)\left(F_{fy'} + F_{ey'}\right) + \frac{d}{2}\left(F_{cx'} + F_{fx'} - F_{dx'} - F_{ex'}\right) + \tau_h \quad (6)$$

where $m = m_h + m_r$ is the human-wheelchair system mass in which m_h is the human mass and m_r is the wheelchair mass; and I_z is the robot moment of inertia about the vertical axis located in G. According to [20], velocities u, ω and $\bar{u}$, including the slip speeds, are given by:

$$u = \frac{r}{2}(\omega_d + \omega_i) \quad (7)$$

$$\omega = \frac{r}{d}(\omega_d - \omega_i) \quad (8)$$

$$\bar{u} = \frac{ar}{d}(\omega_d - \omega_i) \quad (9)$$

where r is the right and left wheel radius; ω_d and ω_i are the angular velocities of the right and left wheels, respectively.

The motor models attained by neglecting the voltage on the inductances are:

$$\tau_d = \frac{k_a(v_d - k_b\omega_d)}{R_a} \; ; \qquad \tau_i = \frac{k_a(v_i - k_b\omega_i)}{R_a} \quad (10)$$

where v_d and v_i are the input voltages applied to the right and left motors; k_a is the torque constant multiplied by the gear ratio; k_b is equal to the voltage constant multiplied by the gear ratio; R_a is the electric resistance constant; τ_d and τ_i are the right and left motor torques multiplied by the gear ratio. The dynamic equations of the motor-wheels are:

$$I_e\dot{\omega}_d + B_e\omega_d = \tau_d - F_{rdx'}R_t \quad (11)$$

$$I_e\dot{\omega}_i + B_e\omega_i = \tau_i - F_{rix'}R_t \quad (12)$$

where I_e and B_e are the moment of inertia and the viscous friction coefficient of the combined motor rotor, gearbox, and wheel, and R_t is the nominal radius of the tire.

In general, most market-available robots have low level PID velocity controllers to track input reference velocities and do not allow the motor voltage to be driven directly. Therefore, it is useful to express the mobile robot model in a suitable way by considering rotational and translational reference velocities as input signals. For this purpose, the velocity controllers are included into the model. To simplify the model, a PD velocity controller has been considered which is described by the following equations:

$$v_u = k_{PT}\left(u_{ref} - u\right) - \dot{u}k_{DT} \quad (13)$$

$$v_\omega = k_{PR}\left(\omega_{ref} - \omega\right) - \dot{\omega}k_{DR} \quad (14)$$

where k_{PT}, k_{DT}, k_{PR} and k_{DR} are gain positive constants of the PD controllers.

From (4 – 14) the following dynamic model of the human-wheelchair system is obtained:

$$\begin{bmatrix} \varsigma_1 & 0 \\ 0 & \varsigma_2 \end{bmatrix}\begin{bmatrix} \dot{u} \\ \dot{\omega} \end{bmatrix} + \begin{bmatrix} \varsigma_4 & \varsigma_3\omega \\ \varsigma_5\omega & \varsigma_6 \end{bmatrix}\begin{bmatrix} u \\ \omega \end{bmatrix} = \begin{bmatrix} u_{ref} \\ \omega_{ref} \end{bmatrix} \tag{15}$$

also, the dynamic equation (15) can be represented as follows,

$$\mathbf{M}(\boldsymbol{\varsigma})\dot{\mathbf{v}} + \mathbf{C}(\boldsymbol{\varsigma}, \mathbf{v})\mathbf{v} = \mathbf{v_{ref}} \tag{16}$$

where $\mathbf{M}(\boldsymbol{\varsigma}) \in \mathcal{R}^{2x2}$ represents the system's inertia, $\mathbf{C}(\boldsymbol{\varsigma}) \in \mathcal{R}^{2x2}$ represents the components of the centripetal forces, $\mathbf{v} \in \mathcal{R}^2$ is the vector of system's velocity; $\mathbf{v_{ref}} \in \mathcal{R}^2$ is the vector of velocity control signals for the wheelchair; and $\boldsymbol{\varsigma} = [\varsigma_1\ \varsigma_2\ \ldots\ \varsigma_6]^T \in \mathcal{R}^6$ is the vector of sistem's dynamic parameters. Hence the properties for the dynamic model with reference velocities as control signals as:

Property 1. Matrix $\mathbf{M}(\boldsymbol{\varsigma})$ is positive definite, additionally it is known that $\|\mathbf{M}(\boldsymbol{\varsigma})\| < k_M$, where, k_M i a positive constant;

Property 2. Furthermore, the following inequalities are also satisfied $\|\mathbf{C}(\boldsymbol{\varsigma}, \mathbf{v})\mathbf{v}\| < k_C\|\mathbf{v}\|$, where, k_C denote a positive constants.

Property 4. The dynamic model of the mobile manipulator can be represented by $\mathbf{M}(\boldsymbol{\varsigma})\dot{\mathbf{v}} + \mathbf{C}(\boldsymbol{\varsigma}, \mathbf{v})\mathbf{v} = \boldsymbol{\Phi}(\mathbf{v})\boldsymbol{\varsigma}$, where, $\boldsymbol{\Phi}(\mathbf{v}) \in \mathcal{R}^{2xl}$ and $\boldsymbol{\varsigma} = [\varsigma_1\ \varsigma_2\ \ldots\ \varsigma_l]^T \in \mathcal{R}^l$ is the vector of l unknown parameters of the human-wheelchair system, *i.e.*, mass of the human, mass of the wheelchair, physical parameters of the wheelchair, motors, velocity, and others.

In order to show the performance of the proposed model dynamic, the identification and validation is shown. The experimental test was implemented on a wheelchair, which admits linear and angular velocities as input reference signals. The identification of the mobile robot was performed by using least squares estimation [21] applied to a filtered regression model [22]. Fig. 2, shown the validation the proposed dynamic model, where it can be seen the good performance of the obtained dynamic model.

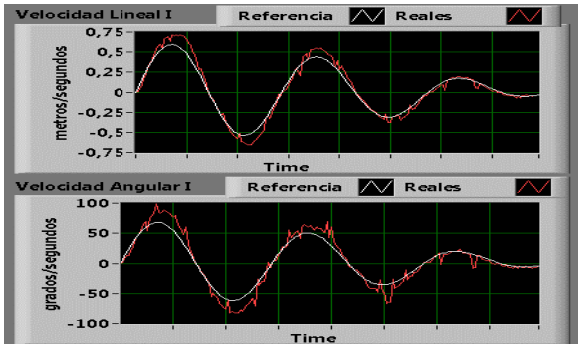

Fig. 2. Validation of the proposed dynamic model

Hence, the full mathematical model of the unicycle-like human-wheelchair system is represented by: (3) the kinematic model and (16) the dynamic model, taking the reference velocities of the robot as input signals.

3 Formulation Problem and Controllers Design

The solution of the path following problem for mobile robots derived in [12] admits an intuitive explanation. A path following controller should aim to reduce to zero both: i) the distance from the vehicle to a point on the path, and ii) the angle between the vehicle velocity vector and the tangent to the path at this point.

3.1 Formulation Problem

As represented in Fig. 3, the path to be followed is denoted as $\mathcal{P}$. The actual desired location $\mathbf{P}_d = [P_{xd} \quad P_{yd}]^T$ is defined as the closest point on $\mathcal{P}$ to the mobile robot, with a desired orientation ψ_d . In Fig. 3, ρ represents the distance between the robot position $\mathbf{h}$ and $\mathbf{P}_d$, and $\tilde{\psi}$ is the error orientation between ψ_d and ψ. Given a path $\mathcal{P}$ in the operational space of the mobile robot and the desired velocity module υ for the robot, the path following problem for mobile robot consists in finding a feedback control law $\mathbf{v}_{\mathbf{ref}}(t) = (s, \upsilon, \rho, \tilde{\psi})$, such that $\lim_{t\to\infty} \rho(t) = 0$ and

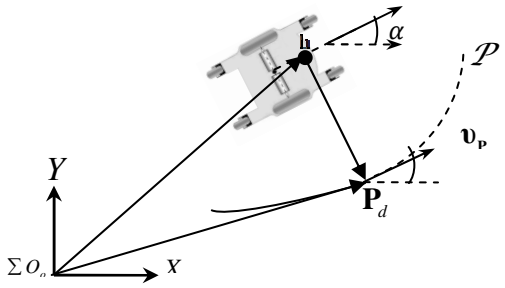

Fig. 3. Schematic of the wheelchair

$\lim_{t\to\infty} \tilde{\psi}(t) = 0$. The error vector of position and orientation between the robot and the point $\mathbf{P}_d$ can be represented as, $\tilde{\mathbf{h}} = \mathbf{P}_d - \mathbf{h}$ and $\tilde{\psi} = \psi_d - \psi$. Therefore, if $\lim_{t\to\infty} \tilde{\mathbf{h}}(t) = \mathbf{0}$ then $\lim_{t\to\infty} \rho(t) = 0$ and $\lim_{t\to\infty} \tilde{\psi}(t) = 0$.

Hence, the desired position and desired velocity of the mobile robot on the path $\mathcal{P}$, are defined as $\mathbf{h_d}(s,h) = \mathbf{P}_d(s,h)$ and $\mathbf{v_{hd}}(s,h) = \boldsymbol{\upsilon}_\mathbf{p}(s,h)$. Where $\boldsymbol{\upsilon}_\mathbf{p}$ is the desired velocity of the robot at location $\mathbf{P}_d$. Note that the component of $\boldsymbol{\upsilon}_\mathbf{p}$ has to be tangent to the trajectory due to kinematics compatibility.

Also, The proposed control scheme to solve the path following problem is shown in Fig. 4, the design of the controller is based mainly on two cascaded subsystems: 1) *Kinematic Controller* with saturation of velocity commands, where the control errors $\rho(t)$ and $\tilde{\psi}(t)$ may be calculated at every measurement time and used to drive the mobile robot in a direction which decreases the errors. Therefore, the control aim is to ensure that $\lim_{t\to\infty} \rho(t) = 0$ and $\lim_{t\to\infty} \tilde{\psi}(t) = 0$; and 2) *Dynamic Compensation Controller*,

which main objective is to compensate the dynamics of the human-wheelchair system, thus reducing the velocity tracking error. The velocity control error is defined as $\tilde{\mathbf{v}} = \mathbf{v_c} - \mathbf{v}$ Hence, the control aim is to ensure that $\lim_{t\to\infty} \tilde{\mathbf{v}}(t) = \mathbf{0}$.

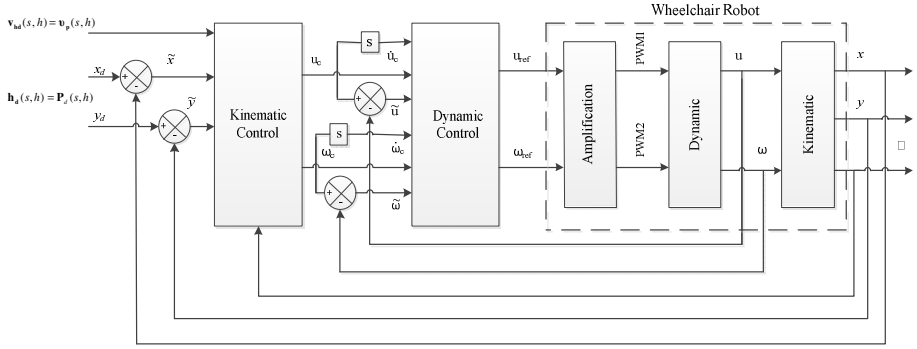

Fig. 4. Dynamic compensation controller: block diagram

3.2 Kinematic and Dynamic Controllers

The proposed kinematic controller is based on the kinematic model of the unicycle-like mobile robot (3), *i.e.*, $\dot{\mathbf{h}} = f(\mathbf{h})\,\mathbf{v}$. Hence following control law is proposed,

$$\begin{bmatrix} u_c \\ \omega_c \end{bmatrix} = \begin{bmatrix} cos\psi & sen\psi \\ -\frac{1}{a}sen\psi & \frac{1}{a}cos\psi \end{bmatrix} \left(\begin{bmatrix} cos\psi_d \\ sen\psi_d \end{bmatrix} + \begin{bmatrix} l_x tanh\left(\frac{k_x}{l_x}\tilde{h}_x\right) \\ l_y tanh\left(\frac{k_y}{l_y}\tilde{h}_y\right) \end{bmatrix} \right) \tag{17}$$

this equation can be written in compact form as,

$$\mathbf{v_c} = \mathbf{J^{-1}}\left(\boldsymbol{\upsilon}_\mathbf{P} + \mathbf{L}\,\mathbf{tanh}\left(\mathbf{L^{-1}K}\,\tilde{\mathbf{h}}\right)\right) \tag{18}$$

where $\tilde{\mathbf{h}} = [\tilde{h}_x \quad \tilde{h}_y]^T$ represents the position error of the wheelchair defined as $\tilde{h}_x = P_{xd} - x$ and $\tilde{h}_y = P_{yd} - y$; $\boldsymbol{\upsilon}_\mathbf{P} = [\upsilon\cos\psi_d \quad \upsilon\sin\psi_d]^T$ is the desired velocity vector on the path; $\mathbf{L}$ and $\mathbf{K}$ are definite positive diagonal matrices that weigh the control error. In order to include an analytical saturation of velocities in the mobile robot, the **tanh**(.) function, which limits the error $\tilde{\mathbf{h}}$, is proposed. The expression $\tanh(\mathbf{L^{-1}K}\,\tilde{\mathbf{h}})$ denote a component by component operation.

Worth noting that the reference desired velocity (t) of the wheelchair during the tracking path need not be constant, with is common in the literature [1,3,13-16],

$$(t) = f(k, \rho(t), \omega(t), \ldots.)$$

the wheelchair's desired velocity can be expressed as: constant function, position error function, angular velocities function of the wheelchair; and the others consideration.

Now, the behaviour of the control position error of the robot is now analyzed assuming -by now- perfect velocity tracking *i.e.,* $\mathbf{v}(t) \equiv \mathbf{v_c}(t)$. By substituting (18) in (3), it is obtained, $\left(\mathbf{v_{hd}} - \dot{\mathbf{h}}\right) + \mathbf{L}\tanh\left(\mathbf{L^{-1}K}\,\tilde{\mathbf{h}}\right) = \mathbf{0}$. Now defining difference signal Υ between $\dot{\mathbf{h}}_\mathbf{d}$ and $\mathbf{v_{hd}}$, *i.e.*, $\Upsilon = \dot{\mathbf{h}}_\mathbf{d} - \mathbf{v_{hd}}$ and remembering that $\dot{\tilde{\mathbf{h}}} = \dot{\mathbf{h}}_\mathbf{d} - \dot{\mathbf{h}}$, it's can be written as

$$\dot{\tilde{\mathbf{h}}} + \mathbf{L}\tanh\left(\mathbf{L^{-1}K}\,\tilde{\mathbf{h}}\right) = \Upsilon \tag{19}$$

For the stability analysis the following Lyapunov candidate function is considered $V\left(\tilde{\mathbf{h}}\right) = \frac{1}{2}\tilde{\mathbf{h}}^\mathbf{T}\tilde{\mathbf{h}} > 0$ Its time derivative on the trajectories of the system is, $\dot{V}\left(\tilde{\mathbf{h}}\right) = \tilde{\mathbf{h}}^\mathbf{T}\Upsilon - \tilde{\mathbf{h}}^\mathbf{T}\mathbf{L}\tanh\left(\mathbf{L^{-1}K}\,\tilde{\mathbf{h}}\right)$. Then, a sufficient condition for $\dot{V}\left(\tilde{\mathbf{h}}\right)$ to be negative definite is,

$$\left|\tilde{\mathbf{h}}^\mathbf{T}\mathbf{L}\tanh\left(\mathbf{L^{-1}K}\,\tilde{\mathbf{h}}\right)\right| > \left|\tilde{\mathbf{h}}^\mathbf{T}\Upsilon\right| \tag{20}$$

Remark 1. $\mathbf{v_{hd}}$ is collinear to $\dot{\mathbf{h}}_\mathbf{d}$, then Υ is also a collinear vector to $\mathbf{v_{hd}}$ and $\dot{\mathbf{h}}_\mathbf{d}$.

Remark 2. For large values of $\tilde{\mathbf{h}}$, it can be considered that: $\mathbf{L}\tanh\left(\mathbf{L^{-1}K}\,\tilde{\mathbf{h}}\right) \approx \mathbf{L}$. $\dot{V}$ will be negative definite only if $\|\mathbf{L}\| > \|\Upsilon\|$; establishing a design condition which makes path following errors $\tilde{\mathbf{h}}$ to decrease

Remark 3. As aforementioned, the desired path velocity can be written as $\mathbf{v_{hd}} = \dot{\mathbf{h}}_\mathbf{d} - \Upsilon$. So, for small values of $\tilde{\mathbf{h}}$, $\mathbf{L}\tanh\left(\mathbf{L^{-1}K}\,\tilde{\mathbf{h}}\right) \approx \mathbf{K}\tilde{\mathbf{h}}$. Thus, the closed loop equation of the system can now written as $\dot{\tilde{\mathbf{h}}} + \mathbf{K}\,\tilde{\mathbf{h}} = \Upsilon$. Applying Laplace representation, one get

$$\tilde{\mathbf{h}}(s) = \frac{1}{s\mathbf{I} + \mathbf{K}}\Upsilon(s) \tag{21}$$

Hence, the direction of the vector of control errors $\tilde{\mathbf{h}}(s)$ tends to the direction of the error velocity vector $\Upsilon(s)$. Therefore, since for finite values $\tilde{\mathbf{h}}(s)$, this location error is normal to $\mathbf{v_{hd}}$ (criterion of minimum distance between the robot and the path), and thus to Υ (see *Remark 1*). Then $\tilde{\mathbf{h}}$ has to be zero. It can now be concluded that $\rho(t) \to 0$ and $\tilde{\psi}(t) \to 0$ for $t \to \infty$ asymptotically.

On the other hand, If there is not considering perfect velocity tracking in kinematic controller design, *i.e.*, $\mathbf{v}(t) \neq \mathbf{v_c}(t)$, the velocity error is defined as, $\tilde{\mathbf{v}}(t) = \mathbf{v_c}(t) - \mathbf{v}(t)$. This velocity error motivates to design of an dynamic compensation controller; the objective of this controller is to compensate the dynamic of the human-wheelchair system, thus reducing the velocity tracking error, hence the following control law dynamic model based (16) is proposed,

$$\begin{bmatrix} u_{ref} \\ \omega_{ref} \end{bmatrix} = \begin{bmatrix} \varsigma_1 & 0 \\ 0 & \varsigma_2 \end{bmatrix} \left(\begin{bmatrix} \dot{u}_c \\ \dot{\omega}_c \end{bmatrix} + \begin{bmatrix} l_u \tanh\left(\frac{k_u}{l_u}\tilde{u}\right) \\ l_\omega \tanh\left(\frac{k_\omega}{l_\omega}\tilde{\omega}\right) \end{bmatrix} \right) + \begin{bmatrix} \varsigma_4 & \varsigma_3\omega \\ \varsigma_5\omega & \varsigma_6 \end{bmatrix} \begin{bmatrix} u \\ \omega \end{bmatrix} \tag{22}$$

Equation (22) can be written in compact form as

$$\mathbf{v_{ref}} = \mathbf{M}(\boldsymbol{\varsigma})\boldsymbol{\sigma}(\tilde{\mathbf{v}}) + \mathbf{C}(\boldsymbol{\varsigma}, \mathbf{v})\mathbf{v} \tag{23}$$

where $\tilde{u} = u_c - u$, $\tilde{\omega} = \omega_c - \omega$ are the linear and angular velocity errors, respectively; $k_u > 0$, $k_\omega > 0$, $l_u > 0$ and $l_\omega > 0$ are positive gain constants.

Next, a Lyapunov candidate function and its time derivative on the system trajectories are introduced in order to consider the corresponding stability analysis $V(\tilde{\mathbf{v}}) = \frac{1}{2}\tilde{\mathbf{v}}^T\tilde{\mathbf{v}}$; the time derivative of the Lyapunov candidate function is,

$$\dot{V}(\tilde{\mathbf{v}}) = \tilde{\mathbf{v}}^T\dot{\tilde{\mathbf{v}}} \tag{24}$$

After introducing the control laws (16) and (23) in (24), the time derivative $\dot{V}(\tilde{\mathbf{v}})$ is now

$$\dot{V}(\tilde{\mathbf{v}}) = -\tilde{\mathbf{v}}^T\boldsymbol{\Gamma}(\tilde{\mathbf{v}}) < 0 \tag{25}$$

$$\dot{V}(\tilde{\mathbf{v}}) = -[\tilde{u} \quad \tilde{\omega}] \begin{bmatrix} l_u & 0 \\ 0 & l_\omega \end{bmatrix} \begin{bmatrix} \tanh\left(\frac{k_u}{l_u}\tilde{u}\right) \\ \tanh\left(\frac{k_\omega}{l_\omega}\tilde{\omega}\right) \end{bmatrix} < 0$$

Hence, it can now be concluded that $\tilde{\mathbf{v}}(t) \to 0$, *i.e.,* $\tilde{u} \to 0$ and $\tilde{\omega} \to 0$ with $t \to \infty$ asymptotically.

4 Experimental Results

In order to show the performance of the proposed controller and dynamic model several experiments were executed. Some of the results are presented in this section. Fig. 5 presents the wheelchair robot used in this work, which has two independently driven wheels by two D.C. motors (in the center part), and four caster wheel to better balance (two in the rear part and two in the front part). Encoders installed on each one of the motor shafts allow knowing the relative position and orientation of the wheelchair.

Information provided by the encoders is used by the PID controllers responsible for getting an independent velocity control of the left and the right wheel.

The experiment corresponds to the control structure shown on Fig. 4. It was implemented on the wheelchair presented on Fig. 5, using the control laws in (18) and (23). Note that for the path following problem, the desired velocity of the wheelchair will depend on the task, the control error, the angular velocity, etc. For this experiment, it is consider that the reference velocity module depends on the control errors. Then, reference velocity in this experiment is expressed as

$$\left|\mathbf{v}_{\mathbf{hd}}\right| = \upsilon_p / (1 + k\rho)$$

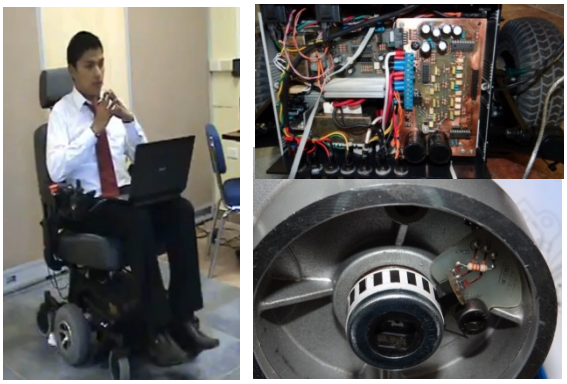

Fig. 5. Autonomous wheelchair

where, k is a positive constant that weigh the control error module. Also, the desired location is defined as the closest point on the path to the wheelchair.

Figures 6-8 show the results of the experiment. Fig. 6 shows the movement on the *X-Y* space. It can be seen that the proposed controller works correctly.

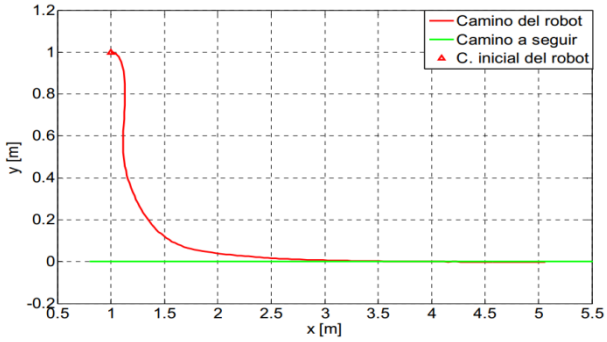

Fig. 6. Movement of the mobile robot based on the experimental data

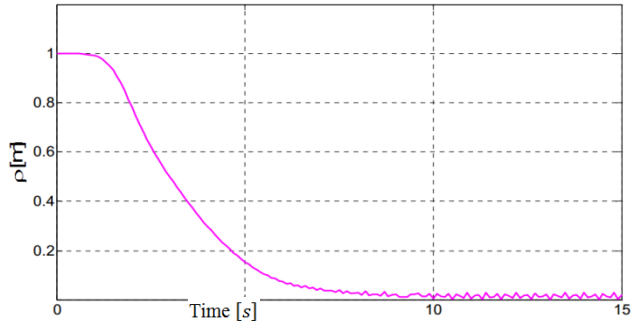

Fig. 7. Distance between the wheelchair and the closest point on the path

Figure 7 shows that $\rho(t)$ remains close to zero, while the Fig. 8 shows the relation between the evolution linear velocity commands and the wheelchair's desired velocity.

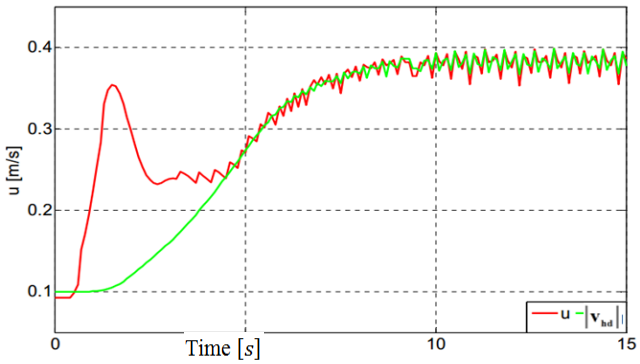

Fig. 8. Linear velocity commands and wheelchair's desired velocity

5 Conclusion

In this work a compensation dynamic controller for solving the path following problem of the human-wheelchair system was proposed. In addition we proposed a dynamic model for the unicycle-like wheelchair, which has reference velocities as control signals to the robot. The design of the whole controller was based on two cascaded subsystems: a kinematic controller which complies with the task objective (path following), and a dynamic controller that compensates the dynamics of the human-wheelchair system. Finally, the stability and robustness are proved by considering the Lyapunov's method, and the performance of the proposed controller is shown through real experiments.

Appendix

The following shows the dynamic parameters of the robotic wheelchair model.

$$\varsigma_1 = \frac{\frac{R_a}{k_a}(2I_e+mrR_t)+2rk_{DT}}{2rk_{PT}} \; ; \varsigma_2 = \frac{\frac{R_a}{k_a}\left(I_e d^2+2rR_t(I_z+a^2m)\right)+2rdk_{DR}}{2rdk_{PR}}$$

$$\varsigma_3 = \frac{\frac{R_a}{k_a}(amR_t)}{2k_{PT}} \quad ; \quad \varsigma_4 = \frac{\frac{R_a}{k_a}\left(\frac{k_a k_b}{R_a}+B_e\right)}{rk_{PT}} + 1; \quad \varsigma_5 = \frac{\frac{R_a}{k_a}(amR_t)}{dk_{PR}} \quad ;$$

$$\varsigma_6 = \frac{\frac{R_a}{k_a}\left(\frac{k_a k_b}{R_a}+B_e\right)d}{2rk_{PR}} + 1.$$

References

1. Bastos-Filho, T., et al.: Towards a New Modality-Independent Interface for a Robotic Wheelchair. IEEE Transactions on Neural Systems and Rehabilitation Engineering 22(3) (2014)
2. Wang, Y., Chen, W.: Hybrid Map-based Navigation for Intelligent Wheelchair. In: IEEE International Conference on Robotics and Automation, China, pp. 637–642 (2011)
3. Cheng, W.-C., Chiang, C.-C.: The Development of the Automatic Lane Following Navigation System for the Intelligent Robotic Wheelchair. In: IEEE International Conference on Fuzzy Systems, Taiwan, pp. 1946–1952 (2011)
4. Abeygunawardhana, P.K.W., Toshiyuki, M.: Self Sustaining Wheelchair Robot on a Curved Trajectory. In: IEEE/ ICIT International Conference on Industrial Technology, pp. 1636–1641 (2006)
5. Biswas, K., Mazumder, O., Kundu, A.S.: Multichannel Fused EMG based Biofeedback System with Virtual reality for Gait Rehabilitation. In: IEEE Proceedings in International Conference on Intelligent Human Computer Interaction, India (2012)
6. Munakata, Y., Tanaka, A., Wada, M.: A Five-wheel Wheelchair with an Active-caster Drive System. In: IEEE International Conference on Rehabilitation Robotics, USA, pp. 1–6 (2013)
7. Yuan, J.: Stability Analyses of Wheelchair Robot Based on Human-in-the-Loop Control Theory. In: IEEE International Conference on Robotics and Biomimetics, Thailand, pp. 419–424 (2009)
8. Soh, H., Demiris, Y.: Involving young children in the development of a safe, smart paediatric wheelchair. Presented at the ACM/IEEE HRI-2011 Pioneers Workshop, Lausanne, Switzerland (2011)
9. Nam, Y., Zhao, Q., Cichocki, A., Choi, S.: Tongue-Rudder: A Glossokinetic-Potential-Based Tongue–Machine Interface. IEEE Transactions on Biomedical Engineering, 290–299 (2012)
10. Munakata, Y., Tanaka, A., Wada, M.: A five-wheel wheelchair with an active-caster drive system. In: IEEE International Conference on Rehabilitation Robotics, pp. 1–6 (2013)
11. De La Cruz, C., Bastos, T.F., Carelli, R.: Adaptive motion control law of a robotic wheelchair. Control Engineering Practice, 113–125 (2011)
12. Soeanto, D., Lapierre, L., Pascoal, A.: Adaptive non-singular path-following, control of dynamic wheeled robots. In: Proceedings of 42nd IEEE Conference on Decision and Control, Hawaii, USA, December 9-12, pp. 1765–1770 (2003)
13. Xu, Y., Zhang, C., Bao, W., Tong, L.: Dynamic Sliding Mode Controller Based on Particle Swarm Optimization for Mobile Robot's Path Following. International Forum on Information Technology and Applications, 257–260 (2009)
14. Wangmanaopituk, S., Voos, H., Kongprawechnon, W.: Collaborative Nonlinear Model-Predictive Collision Avoidance and Path Following of Mobile Robots. In: ICROS-SICE International Joint Conference 2009, Japan, pp. 3205–3210 (2009)
15. Tanimoto, Y., Yamamoto, H., Namba, K., Tokuhiro, A., Furusawa, K., Ukida, H.: Imaging of the turn space and path of movement of a wheelchair for remodeling houses of individuals with SCI. In: IEEE International Conference on Imaging Systems and Techniques (2012)
16. Chen, S.-H., Chou, J.-J.: Motion control of the electric wheelchair powered by rim motors based on event-based cross-coupling control strategy. In: IEEE/SICE International Symposium on System Integration (2011)

17. Martins, F.N., Celeste, W., Carelli, R., Sarcinelli-Filho, M., Bastos-Filho, T.: An Adaptive Dynamic Controller for Autonomous Mobile Robot Trajectory Tracking. Control Engineering Practice 16, 1354–1363 (2008)
18. Chénier, F., Bigras, P., Aissaoui, R.: A new dynamic model of the manual wheelchair for straight and curvilinear propulsion. In: IEEE International Conference on Rehabilitation Robotics (2011)
19. Yahaya, S.Z., Boudville, R., Taib, M.N., Hussain, Z.: Dynamic modeling and control of wheel-chaired elliptical stepping exercise. In: IEEE International Conference on Control System, Computing and Engineering, pp. 204–209 (2012)
20. Zhang, Y., Hong, D., Chung, J.H., Velinsky, S.A.: Dynamic Model Based Robust Tracking Control of a Differentially Steered Wheeled Mobile Robot. In: Proceedings of the American Control Conference, Philadelphia, Pennsylvania, pp. 850–855 (1998)
21. Aström, K.J., Wittenmark, B.: Adaptive Control. Addison-Wesley (1995)
22. Reyes, F., Kelly, R.: On parameter identification of robot manipulator. In: IEEE International Conference on Robotics and Automation, pp. 1910–1915 (1997)